

Molecular diversity of Ca²⁺ channel α_1 subunits from the marine ray *Discopyge ommata*

W. A. HORNE*†, P. T. ELLINOR‡, I. INMAN‡, M. ZHOU*†, R. W. TSIE‡, AND T. L. SCHWARZ‡§

†Department of Molecular and Cellular Physiology, Stanford University Medical Center, Stanford, CA 94305; and *Department of Pharmacology, College of Veterinary Medicine, Cornell University, Ithaca, NY 14850

Communicated by James A. Spudich, January 7, 1993

ABSTRACT In many neurons, transmitter release from presynaptic terminals is triggered by Ca²⁺ entry via dihydropyridine-insensitive Ca²⁺ channels. We have looked for cDNAs for such channels in the nervous system of the marine ray *Discopyge ommata*. One cDNA (doe-2) is similar to dihydropyridine-sensitive L-type channels, and two cDNAs (doe-1 and doe-4) are more similar to the subfamily of dihydropyridine-insensitive non-L-type channels. doe-4, which encodes a protein of 2326 aa, most closely resembles a previously cloned N-type channel. doe-1, which encodes a protein of 2223 aa, is a member of a separate branch of the non-L-type channels. Northern blot analysis reveals that doe-1 is abundant in the forebrain. doe-4 is more plentiful in the electric lobe and, therefore, may control neurotransmitter release in motor nerve terminals. These results show that the familial pattern of Ca²⁺-channel genes has been preserved from a stage in evolution before the divergence of higher and lower vertebrates >400 million years ago. The cloning of these channels may be a useful starting point for elucidating the role of the Ca²⁺ channels in excitation–secretion coupling in nerve terminals.

Delineation of the molecular diversity of voltage-gated Ca²⁺ channels is essential for understanding how these channels control a wide spectrum of cellular functions ranging from secretion and contraction to metabolism and gene expression. Several types of voltage-gated Ca²⁺ channels (L, T, N, and P types) have been distinguished by functional criteria and show different tissue distributions and differential sensitivity to modulators and drugs (1, 2). Much of the known diversity among Ca²⁺ channels may arise from the existence of multiple forms of the α_1 subunit (3–10), which are large (200–260 kDa) transmembrane proteins and are responsible for Ca²⁺-channel voltage dependence, selectivity for Ca²⁺, and sensitivity to pharmacological modulation.

Two structural subfamilies of α_1 subunits have emerged from molecular cloning of mammalian cDNAs (11, 12). The first subfamily includes α_1 cDNAs originally derived from skeletal muscle (3, 13), heart (4), aorta (14), lung (15), and brain (7, 8). Expression of these channels demonstrated that they are responsive to 1,4-dihydropyridines (DHPs) and may thus be classified as L-type channels. The second α_1 subfamily consists so far of cDNAs derived from mammalian brain. The individuals within this subfamily show upward of 60% identity with each other but only \approx 45% with members of the first subfamily (5, 6, 9, 10), and, when expressed, lack the characteristic DHP response of L-type channels (5, 10).

We chose the marine ray *Discopyge ommata* as a source for additional neuronal Ca²⁺-channel cDNAs. The electric organ of marine rays has served as a valuable model system for studying the biochemical properties of synaptic proteins. The nerve terminals within the electric organ of *D. ommata* are the richest known source of receptors for the cone snail

```
doe-1  IGMQVFGNIQLDDHTFIRNRNNNFSTFFNALMLLFRSATGESWQ
rbB    IGMQVFGNIALDDGTSINRNNNFRTFFQALMLLFRSATGEAWH
L1 (skel) IGMQVFGKIALVDGTQINRNNNFQTFPQAVLLLFRCATGEAWQ
L2 (card) IGMQVFGKIALNDTTEINRNNNFQTFPQAVLLLFRCATGEAWQ
L3 (neur) IGMQVFGKIAMRDNINRNNNFQTFPQAVLLLFRCATGEAWQ
doe-2  IGMQVFGKIALVDGTQINRNNNFQTFPQAVLLLFRCATGEAWQ
```

FIG. 1. PCR-derived Ca²⁺-channel fragments from *D. ommata* fall into both subfamilies of high-voltage-activated channels. The fragments are from the region after IVS5. The sequences encoded by the oligonucleotides for PCR are marked with arrows; the position of the detection oligonucleotide is marked with a dashed line. Residues that differ from the sequence of the skeletal muscle L₁ channel are shaded. doe-1 is grouped with the DHP-insensitive rbB channel from rat brain (9, 11); doe-2 is grouped with the DHP-sensitive L-type channels (3–8).

toxin ω -conotoxin GVIA (16), a selective probe for N-type Ca²⁺ channels. Here we report the molecular cloning of two full-length cDNAs that encode putative Ca²⁺-channel α_1 subunits[¶] that are differentially expressed in the forebrain and in the electric lobe that innervates the electric organ.

METHODS

PCR and Molecular Cloning. Phage template DNA was isolated from plate lysates (17) of an oligo(dT)-primed λ gt10 cDNA library (kindly provided by F. Rupp and R. Scheller, Stanford University). Forty cycles of PCR (95°C for 1 min, 52°C for 2 min, and 72°C for 1 min) were performed using standard conditions (17). PCR products were separated through a 1.2% agarose gel, transferred to Hybond membranes (Pharmacia), and hybridized with a ³²P-end-labeled degenerate oligonucleotide probe (see Results). Positive DNA fragments were gel-purified, blunt-ended with T4 DNA polymerase, phosphorylated with T4 polynucleotide kinase, and ligated into the *Sma* I site of pBluescript SK+ (Stratagene). Plasmid DNA was purified and sequenced by the dideoxynucleotide termination method (18). Ca²⁺-channel cDNAs were isolated from the oligo(dT)-primed λ gt10 library from electric lobe and additional randomly and specifically primed forebrain and electric lobe cDNA libraries in λ ZAP II (Stratagene). Libraries were probed with the PCR-derived clones or successive cDNA isolates. DNA sequencing was performed by creating nested deletions on both strands (Promega Erase-A-Base) and with specifically synthesized primers. Sequence analysis was carried out using GCG software (19).

Isolation of RNA and Northern Blot Analysis. Poly(A)⁺ RNA was isolated from either forebrain or electric lobe regions of *D. ommata* by using the guanidinium isothiocya-

Abbreviation: DHP, dihydropyridine.

†Present address: Neurex Corp., 3760 Haven Avenue, Menlo Park, CA 94025.

§To whom reprint requests should be addressed.

¶The sequences reported in this paper have been deposited in the GenBank data base [accession nos. L12531 (doe-1) and L12532 (doe-4)].

The publication costs of this article were defrayed in part by page charge payment. This article must therefore be hereby marked "advertisement" in accordance with 18 U.S.C. §1734 solely to indicate this fact.

doe-1	MARFGA	EVGSL	SADAS	SEGRSR	HQVPT	GETAV	AAAA	AAVVA	GAAG	GSAG	KQTR	AQRART	MAAL	YNP	IPV	RNC	LANR	SFLF	GEDN	IVNR	SABR	RVIE	100		
BI-2	MARFGD	EMPA	RYGGG	GAGAA	AGVTV	VGAA	GRRG	GAGS	ROGG	OGG	GAORMY	KQSM	AQRART	MAAL	YNP	IPV	RNC	LANR	SFLF	SEDM	IVNR	KRYAK	ITE	96	
rbB	MURFGD	ELGG	RYGGT	GAGGERA	...	RGGG	GAGG	PGGG	GGGL	GGOR	VLYV	KOST	AQRART	MAAL	YNP	IPV	RNC	LANR	SFLF	SEDM	IVNR	KRYAK	ITE	93	
doe-4	MARFGD	NDVFA	CYGGSP	AG	...	GGFG	ANRHA	QAG	OGMY	GS	SS	LAOR	ARTMA	AL	YNP	IPV	RNC	LANR	SFLF	SEDM	IVNR	KRYAK	ITE	86	
doe-1	WPFPEY	MILATI	IANCV	LAL	EQHLP	MDKTP	MAKSL	EQTE	YF	IG	IFC	FEAG	IKI	AL	GV	FH	KGSY	LRNG	WN	MD	FV	VV	LT	200	
BI-2	WPFPEY	MILATI	IANCV	LAL	EQHLP	DDKTP	MSER	LD	TE	YF	IG	IFC	FEAG	IKI	AL	GV	FH	KGSY	LRNG	WN	MD	FV	VV	LT	196
rbB	WPFPEY	MILATI	IANCV	LAL	EQHLP	DDKTP	MSER	LD	TE	YF	IG	IFC	FEAG	IKI	AL	GV	FH	KGSY	LRNG	WN	MD	FV	VV	LT	193
doe-4	WPFPEY	MILATI	IANCV	LAL	EQHLP	DDKTP	MSER	LD	TE	YF	IG	IFC	FEAG	IKI	AL	GV	FH	KGSY	LRNG	WN	MD	FV	VV	LT	186
doe-1	VRVLRP	LKLV	SGIP	SLOV	VV	LKSI	MKAM	VPLL	QIGL	LL	FFAI	LMFA	IIGLE	FY	YGR	LR	TCY	TD	DA	AA	AE	ELD	LQ	299	
BI-2	VRVLRP	LKLV	SGIP	SLOV	VV	LKSI	MKAM	VPLL	QIGL	LL	FFAI	LMFA	IIGLE	FY	YGR	LR	TCY	TD	DA	AA	AE	ELD	LQ	296	
rbB	VRVLRP	LKLV	SGIP	SLOV	VV	LKSI	MKAM	VPLL	QIGL	LL	FFAI	LMFA	IIGLE	FY	YGR	LR	TCY	TD	DA	AA	AE	ELD	LQ	292	
doe-4	VRVLRP	LKLV	SGIP	SLOV	VV	LKSI	MKAM	VPLL	QIGL	LL	FFAI	LMFA	IIGLE	FY	YGR	LR	TCY	TD	DA	AA	AE	ELD	LQ	284	
doe-1	GITFND	NILFA	LVTF	VQCIT	MEG	WTD	I	LYNT	ND	AL	GNT	WN	WLY	F	I	P	L	I	I	G	S	F	F	399	
BI-2	GITFND	NILFA	LVTF	VQCIT	MEG	WTD	I	LYNT	ND	AL	GNT	WN	WLY	F	I	P	L	I	I	G	S	F	F	396	
rbB	GITFND	NILFA	LVTF	VQCIT	MEG	WTD	I	LYNT	ND	AL	GNT	WN	WLY	F	I	P	L	I	I	G	S	F	F	392	
doe-4	GITFND	NILFA	LVTF	VQCIT	MEG	WTD	I	LYNT	ND	AL	GNT	WN	WLY	F	I	P	L	I	I	G	S	F	F	384	
doe-1	DKAEV	MIL	EAED	KN	AEK	SAL	H	V	L	R	A	T	K	K	R	M	E	M	T	T	S	S	E	498	
BI-2	SKAEV	MIL	EAED	KN	AEK	SAL	H	V	L	R	A	T	K	K	R	M	E	M	T	T	S	S	E	495	
rbB	DKAEV	MIL	EAED	KN	AEK	SAL	H	V	L	R	A	T	K	K	R	M	E	M	T	T	S	S	E	491	
doe-4	DKAEV	MIL	EAED	KN	AEK	SAL	H	V	L	R	A	T	K	K	R	M	E	M	T	T	S	S	E	480	
doe-1	LVALN	TCV	AV	VH	YD	Q	P	L	W	S	N	F	L	Y	A	E	F	L	G	L	F	S	S	598	
BI-2	LVALN	TCV	AV	VH	YD	Q	P	L	W	S	N	F	L	Y	A	E	F	L	G	L	F	S	S	595	
rbB	LVALN	TCV	AV	VH	YD	Q	P	L	W	S	N	F	L	Y	A	E	F	L	G	L	F	S	S	591	
doe-4	LVALN	TCV	AV	VH	YD	Q	P	L	W	S	N	F	L	Y	A	E	F	L	G	L	F	S	S	580	
doe-1	YWSLR	NLV	SV	LL	SM	KSI	I	IS	LL	FL	FL	FI	VV	F	AL	L	G	M	Q	L	F	G	G	698	
BI-2	YWSLR	NLV	SV	LL	SM	KSI	I	IS	LL	FL	FL	FI	VV	F	AL	L	G	M	Q	L	F	G	G	695	
rbB	YWSLR	NLV	SV	LL	SM	KSI	I	IS	LL	FL	FL	FI	VV	F	AL	L	G	M	Q	L	F	G	G	691	
doe-4	YWSLR	NLV	SV	LL	SM	KSI	I	IS	LL	FL	FL	FI	VV	F	AL	L	G	M	Q	L	F	G	G	680	
doe-1	VTLTF	GN	YLL	NV	LAI	AV	DN	LANA	QEL	T	K	DEE	E	E	E	E	E	E	E	E	E	E	793		
BI-2	VTLTF	GN	YLL	NV	LAI	AV	DN	LANA	QEL	T	K	DEE	E	E	E	E	E	E	E	E	E	E	795		
rbB	VTLTF	GN	YLL	NV	LAI	AV	DN	LANA	QEL	T	K	DEE	E	E	E	E	E	E	E	E	E	E	789		
doe-4	VTLTF	GN	YLL	NV	LAI	AV	DN	LANA	QEL	T	K	DEE	E	E	E	E	E	E	E	E	E	E	779		
doe-1	TD	...	AL	GL	EG	S	R	Y	R	R	R	S	R	I	F	A	...	ES	L	R	I	A	875		
BI-2	SEMDP	ER	L	W	A	S	T	A	R	H	R	P	D	M	K	T	H	L	D	R	L	V	V	889	
rbB	SEMDP	ER	L	W	A	S	T	A	R	H	R	P	D	M	K	T	H	L	D	R	L	V	V	881	
doe-4	SEMDP	ER	L	W	A	S	T	A	R	H	R	P	D	M	K	T	H	L	D	R	L	V	V	869	
doe-1	VEAGS	F	R	M	A	E	P	I	R	A	R	R	R	S	L	K	E	A	M	G	L	E	S	949	
BI-2	QEAEL	S	R	E	G	Y	G	R	E	S	D	H	A	R	E	G	L	E	P	P	G	E	A	979	
rbB	TEFGA	R	E	R	R	K	R	S	H	S	K	E	A	P	G	...	AD	T	Q	V	R	...	978		
doe-4	PRNS	K	D	D	K	R	C	S	H	S	K	E	A	P	G	...	AD	T	Q	V	R	...	949		
doe-1	OMKAF	S	W	G	E	P	H	S	S	M	T	R	P	D	V	T	D	P	S	G	N	L	1041		
BI-2	ERRR	H	R	H	R	G	S	P	A	R	S	G	E	A	E	P	D	G	G	G	G	G	1068		
rbB	ERRR	H	R	H	R	G	S	P	A	R	S	G	E	A	E	P	D	G	G	G	G	G	1048		
doe-4	ERRR	H	R	H	R	G	S	P	A	R	S	G	E	A	E	P	D	G	G	G	G	G	1041		
doe-1	IDV	C	E	N	T	E	T	P	M	D	S	1055			
BI-2	EPL	A	E	D	M	N	L	K	S	P	A	E	P	S	P	H	E	N	L	S	H	A	1168		
rbB	VDE	P	E	D	A	D	N	K	N	I	V	L	P	1089			
doe-4	LEQ	P	E	D	A	D	N	K	N	I	V	L	P	1084			
doe-1	1120			
BI-2	TAR	P	D	H	T	T	V	E	I	P	P	A	C	P	P	L	N	H	T	V	V	Q	1268		
rbB	1163			
doe-4	1162			
doe-1	ALAAE	P	V	Q	P	A	R	N	N	V	L	K	Y	D	V	F	T	G	V	F	T	F	1220		
BI-2	ALAAE	P	V	Q	P	A	R	N	N	V	L	K	Y	D	V	F	T	G	V	F	T	F	1365		
rbB	ALAAE	P	V	Q	P	A	R	N	N	V	L	K	Y	D	V	F	T	G	V	F	T	F	1263		
doe-4	ALAAE	P	V	Q	P	A	R	N	N	V	L	K	Y	D	V	F	T	G	V	F	T	F	1258		
doe-1	IKRLP	K	L	K	A	V	D	C	V	V	N	L	N	L	I	V	Y	M	L	F	M	F	1319		
BI-2	IKRLP	K	L	K	A	V	D	C	V	V	N	L	N	L	I	V	Y	M	L	F	M	F	1465		
rbB	IKRLP	K	L	K	A	V	D	C	V	V	N	L	N	L	I	V	Y	M	L	F	M	F	1363		
doe-4	IKRLP	K	L	K	A	V	D	C	V	V	N	L	N	L	I	V	Y	M	L	F	M	F	1358		
doe-1	STGEG	W	P	Q	V	L	K	H	S	V	D	A	T	E	F	1419			
BI-2	STGEG	W	P	Q	V	L	K	H	S	V	D	A	T	E	F	1565			
rbB	STGEG	W	P	Q	V	L	K	H	S	V	D	A	T	E	F	1463			
doe-4	STGEG	W	P	Q	V	L	K	H	S	V	D	A	T	E	F	1458			
doe-1	YR	M	Q	F	V	V	S	P	F	E	Y	T	L	M	A	L	N	T	V	L	M	K	1519		
BI-2	YR	M	Q	F	V	V	S	P	F	E	Y	T	L	M	A	L	N	T	V	L	M	K	1665		
rbB	YR	M	Q	F	V	V	S	P	F	E	Y	T	L	M	A	L	N	T	V	L	M	K	1563		
doe-4	YR	M	Q	F	V	V	S	P	F	E	Y	T	L	M	A	L	N	T	V	L	M	K	1558		

FIG. 2. (Figure continues on the opposite page.)



Fig. 2. Alignment of the deduced amino acid sequences of doe-1 and doe-4 with representative mammalian clones of the non-L subfamily [rbB (9) and BI-2, the longer variant of the BI type (5)]. Dots represent gaps introduced by the BESTFIT program (GCG) to optimize alignment. When two or more residues at a position are identical, they are boxed. If two pairs of boxes are possible at a single position, the pair is boxed that includes the doe-4 sequence. The predicted positions of transmembrane (S1–S6) and pore-forming (H5) regions in each of the homologous repeats (I–IV) are indicated by brackets below. The position of an insert encountered in some doe-4 clones is indicated by a solid triangle. Predicted glycosylation sites in either doe-1 or doe-4 are indicated by open triangles. Potential sites for phosphorylation are marked by solid circles (cAMP-dependent protein kinase), open circles (protein kinase C), and plus marks (multifunctional Ca²⁺/calmodulin-dependent protein kinase).

nate method and selection on oligo(dT) resin (17). Poly(A)⁺ RNA (3 μg) from each tissue was electrophoresed through a 1% agarose/0.8% formaldehyde gel and transferred to a nylon membrane for hybridization (17).

RESULTS AND DISCUSSION

Molecular Cloning. We used PCR to amplify candidate Ca²⁺-channel cDNA sequences from a cDNA library derived from the electric lobe of *D. ommata*. Degenerate primers were synthesized based on amino acid sequences, IGMQ-(V/M)FG and ATGEAW(Q/H), flanking 29 aa in the region between transmembrane domains IVS5 and IVS6 (Fig. 1). To identify putative Ca²⁺-channel sequences, the PCR products were probed with an oligonucleotide based on a sequence, INR(N/H)NNF, within the predicted amplified region. DNA sequencing of positive clones yielded two distinct 128-bp fragments [*D. ommata*-1 (doe-1) and doe-2]. Sequence alignment indicates that doe-2 is as homologous to Ca²⁺ channels from skeletal muscle or heart as these L-type channels are to each other. Within this limited region of 29 aa, the doe-2 fragment differs from the skeletal muscle sequence at only 3 aa positions (Fig. 1).

In contrast, the doe-1 fragment is less closely related to L-type channels and much more similar to a Ca²⁺-channel clone from rat brain (rbB; ref. 11). Starting with the doe-1

PCR fragment, we isolated overlapping cDNAs encoding the complete open reading frame (Fig. 2). The screening procedure also led to isolation of a distinct class of cDNA encoding doe-4, an additional putative Ca²⁺ channel. The doe-1 sequence consists of an open reading frame of 6669 bp, encoding a protein of 2223 aa with a calculated molecular mass of 251.8 kDa. doe-4 consists of an open reading frame of 6978 bp, corresponding to a protein of 2326 aa and a calculated molecular mass of 264.5 kDa. Like other Ca²⁺-channel α₁ subunits (3), doe-1 and doe-4 consist of four largely hydrophobic repeats (I–IV), separated by largely hydrophilic linkers. Each repeat includes an H5 region, which is thought to line the conduction path, and six putative transmembrane segments (S1–S6).

In analyzing doe-4 cDNA, we repeatedly encountered a variant of the loop that joins the first two homology domains, a region that is otherwise well-conserved among this family of channels. This variation is likely to arise from alternative splicing and results in the insertion of a 20-aa sequence (DGLGIYEPEQKPEDIQSVY) at a position marked in Fig. 2. Potential sites for phosphorylation by protein kinases are also marked. Because Ca²⁺ channels undergo physiological modulations by several second messenger systems (20, 21), these sites are potentially significant.

Distribution of mRNAs. Northern blot analysis of the tissue distribution of doe-1 and doe-4 mRNAs is illustrated in Fig.

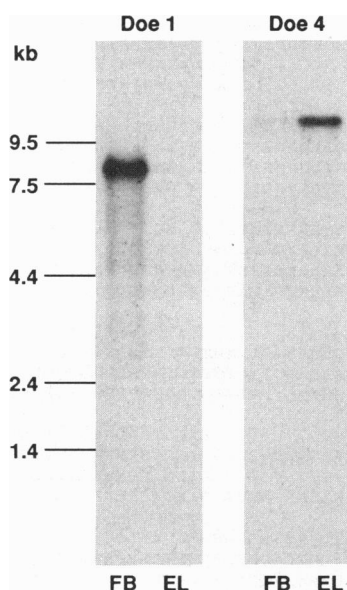


FIG. 3. Differential expression of *doe-1* and *doe-4* transcripts in the central nervous system of *D. ommata*. Poly(A)⁺ RNA (3 μ g per lane) from the forebrain (lanes FB) or electric lobe (lanes EL) were probed with ³²P-labeled cDNA from regions likely to be specific for the individual gene (the 5' untranslated region of *doe-1* or the cytoplasmic linker between repeats II and III of *doe-4*). Size standards from an RNA ladder (BRL) are indicated at the left.

3. *doe-1*, an 8-kb transcript, is much more abundant in forebrain than in the electric lobe; in contrast, *doe-4*, a 12- to 13-kb transcript, is more plentiful in electric lobe than in forebrain. Since the electric lobe consists largely of the electromotor nucleus which innervates the electric organ, this suggests that *doe-4* may play an important role in regulating transmitter release from motor nerve terminals. Consistent with this hypothesis, neurotransmitter release in the electric organ is blocked by ω -conotoxin GVIA (16), which also blocks the human homolog of clone *rbB* (10).

Relationships to Previously Described Ca²⁺-Channel Structures. Fig. 4 provides an overview of structural homologies between *doe-1* and *doe-4* and mammalian Ca²⁺-channel cDNAs (see below). The tree diagram is based on sequence homology, but it also appears representative of an emerging pattern of functional differences. The upper branch consists of three α_1 genes designated as L₁, L₂, and L₃ (1, 12). To date, the Ca²⁺-channel activity expressed from members of this group has displayed responses to DHP antagonists and agonists and other functional characteristics expected for L-type Ca²⁺ channels. Individual members of this L subfamily display at least 60–70% amino acid identity with each other.

Members of the second subfamily show only \approx 40% amino acid identity with members of the L subfamily but >60% homology with each other. They are functionally distinct from the L subfamily in several respects (1). Most notably, they encode high-voltage-activated Ca²⁺ channels that are not inhibited by DHP antagonists or stimulated by DHP agonists (5, 10). By grouping the nearly identical genes from different species, three types of mammalian channels can be distinguished within this subfamily. They are represented by clones BI (*rbA*, CaCh4) (5, 6, 11, 12) and BII (22), which were isolated from rabbit brain, and *rbB* (CaCh5) (9–12), which was cloned from rat brain. The BI cDNA encodes an α_1 subunit with some key features expected for P-type Ca²⁺ channels, which are highly expressed in cerebellar Purkinje cells and certain nerve terminals (5). The *rbB* cDNA encodes an ω -conotoxin-sensitive, DHP-resistant activity character-

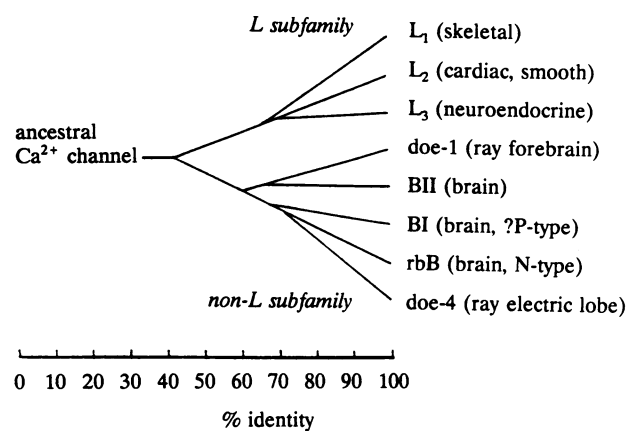


FIG. 4. Structural homologies of the mammalian and marine ray Ca²⁺-channel α_1 subunits. Percent sequence identity, as determined by the BESTFIT program using the full amino acid sequence, is indicated. The subfamily of L-type channels is represented by L₁ from rabbit skeletal muscle, L₂ from rabbit cardiac muscle, and L₃ from human brain. *doe-2* is not included because a comparable percent identity could not be determined from the limited sequence available. The subfamily of non-L channels includes *doe-4*, *rbB* (an N-type channel from rat brain; ref. 9), and BI (a rabbit cerebellar channel with some similarity to the P-type channel; ref. 5) and the more distantly related *doe-1*. In the nomenclature for mammalian brain channels of Snutch *et al.* (11), channels like L₂ are class C, those like L₃ are class D, those like BI are class A, and those like *rbB* are class B.

istic of an N-type Ca²⁺ channel (9, 10). The recently reported BII channel has not been physiologically characterized (22).

doe-1 and *doe-4* belong to the non-L subfamily. The degree of homology to BI or *rbB* clones ranges between 60 and 72% identity; in contrast, the homology between *doe-1* or *doe-4* and various L-type Ca²⁺ channels is <45%. Some distinguishing structural features now emerge from a comparison of the L and non-L subfamilies. In contrast to all known L-type channels, for example, *doe-1*, *doe-4*, and BI or *rbB* cDNAs encode proteins containing an extra positive charge in repeat III (Fig. 5A) and a different pattern of spacing of charged residues in repeat IV (Fig. 5B). Similar considerations hold for the cytoplasmic loop between repeats III and IV (Fig. 5C), a segment thought to be important for inactivation (23, 24). *doe-1*, *doe-4*, BI, and *rbB* are highly homologous along this stretch but display significant differences with respect to L-type channel cDNAs.

From sequence analysis, we suggest that *doe-1* and BII, which are 68% identical, represent a distinct branch of the non-L subfamily. The deduced amino acid sequence of *doe-1* shows somewhat less identity to BI and *rbB* than they do to each other. The overall identities are 60% for *doe-1* and *rbB*, 63% for *doe-1* and BI, and 68% for BI and *rbB*. The most striking sequence divergence between *doe-1* and the other branch of the non-L subfamily occurs in the cytosolic loop between repeats II and III.

doe-4 can more easily be grouped with BI and *rbB* than with *doe-1* and BII (68, 72, 61, and 61% identities, respectively). In particular, where the subfamily shows the greatest divergence, some regions of *doe-4* appear especially similar to *rbB*. This is most striking in the C termini of the channels: *rbB* and *doe-4* extend, respectively, 174 and 185 aa beyond the end of BI and are identical to each other at 110 of these residues. Similar comparison can be made in the cytoplasmic linker between domains II and III.

CONCLUSIONS

From a comparison of sequences, the *doe-1* channel reported here and the mammalian BII clone (22) can be recognized as

A	doe-1	IKSLRVLRLRPLKTIKRL	B	doe-1	LSFLKLFRAARLIKLLRQD
	doe-4	IKSLRVLRLRPLKTIKRL		doe-4	LSFLRLFRFAARLIKLLRQD
	B1	IKSLRVLRLRPLKTIKRL		B1	LSFLRLFRFAARLIKLLRQD
	rbB	IKSLRVLRLRPLKTIKRL		rbB	LSFLRLFRFAARLIKLLCRQD
	L ₂	VKILRVLRLRPLRAINRA		L ₂	ITFFRLFRVMRLVKLLSRG
	L ₁	VKILRVLRLRPLRAINRA		L ₁	SAFFRLFRVMRLIKLLSRA
C	doe-1	ITFQEQGDKMLEESSLEKNERACIDFAISAKPLTRYMPQNRQTFQYRVWQFVVSF			
	doe-4	ITFQEQGDKVMSDCSLEKNERACIDFAISAKPLTRYMPQNKQTFQYKMWKFFVVSF			
	B1	ITFQEQGDKMEEYSLEKNERACIDFAISAKPLTRHMPQNKQSFQYRMWQFVVSF			
	rbB	ITFQEQGDKVMSECSLEKNERACIDFAISAKPLTRYMPQNKQSFQYKWTFFVVSF			
	L ₂	VTFQEQGEQYKNCLELDKNQRQCVEYALKARPLRRYIE--KNHQHYVWVYVNST			
	L ₁	VTFQEQGETEYKNCLELDKNQRQCQYALKARPLRCYIE--KNPYQYQVWVYVNST			

Fig. 5. Comparison of motifs between representatives of the L and non-L subfamilies. (A) IIIS4. (B) IVS4. (C) III/IV linker. (A and B) The positively charged repeating residues have been shaded to highlight the additional charge in IIIS4 and the shifted spacing in IVS4 that appear to distinguish members of the non-L family from the L family. (C) The sequence of doe-1 and any matches to its sequence have been shaded to illustrate the structural similarities of the non-L family that diverge from the L-type channels.

a distinct branch of the non-L subfamily of Ca²⁺ channels. We have also cloned a Ca²⁺ channel (doe-4) that is likely to play a role in transmitter release from terminals in the electric organ and is likely to correspond to the ω -conotoxin binding protein that we (25) and others (16) have studied. The electric organ channel is of special interest because of the high density of synapses in this tissue. The sequence of a channel that may be a component of the presynaptic release site in this organ (16) will be a useful tool in the purification of presynaptic plasma membranes and for elucidating the role of the Ca²⁺ channels in vesicle docking and fusion (26).

Analysis of the marine ray Ca²⁺ channels has provided some evolutionary perspectives on Ca²⁺-channel diversity. Marine rays are cartilaginous fish and diverged from animals with bony skeletons >4 × 10⁸ years ago. doe-2 represents a Ca²⁺ channel homologous to members of the mammalian L-type subfamily, whereas doe-1 and doe-4 fit within the non-L subfamily. Evidently, L-type and non-L-type subfamilies separated before the divergence between cartilaginous and higher vertebrates, hundreds of millions of years ago. Interestingly, homology analysis of Na⁺ channels points toward the opposite relationship; the electric-eel Na⁺ channel appears to have branched away from the mammalian genes before the major division of mammalian Na⁺ channels into muscle types and neuronal types (27). Among K⁺ channels, divisions into subgroups appear to be very ancient; classes have been conserved between *Drosophila* and mammals (28). Physiologic studies indicate that the division of Ca²⁺ channels may also be that old; both DHP-sensitive and DHP-insensitive Ca²⁺ channels have been described in *Aplysia* and *Drosophila* (29, 30).

Sequence comparisons of doe-1, doe-4, and mammalian clones have provided information regarding the structural properties of voltage-gated Ca²⁺ channels. These comparisons highlight structural domains, both conserved and divergent, that could play key roles in providing functional diversity among Ca²⁺-channel subtypes. For example, the presence of an extra positive charge in the III S4 region of non-L type channels may be related to findings of a steeper voltage dependence of activation of expressed channels. By analogy to excitation-contraction coupling in skeletal muscle, which depends critically on the II-III loop (31), variability in the II-III loop and the C-terminal tail of neuronal structures might allow the various Ca²⁺ channels to play distinct roles in excitation-secretion coupling.

We thank Elyse Jung and Jackie Phillips for technical assistance. This work was supported by National Institutes of Health Grants GM42376 (T.L.S.) and NS24067 (R.W.T.) and gifts from Miles, Parke-Davis, Wyeth-Ayerst, and Eli Lilly (R.W.T.).

1. Tsien, R. W., Ellinor, P. T. & Horne, W. A. (1991) *Trends Pharmacol. Sci.* **12**, 349-354.
2. Snutch, T. P. & Reiner, P. B. (1992) *Curr. Opin. Neurobiol.* **2**, 247-253.
3. Tanabe, T., Takeshima, H., Mikami, A., Flockerzi, V., Takahashi, H., Kangawa, K., Kojima, M., Mitsu, H., Hirose, T. & Numa, S. (1987) *Nature (London)* **328**, 313-318.
4. Mikami, A., Imoto, K., Tanabe, T., Niidome, T., Mori, Y., Takeshima, H., Narumiya, S. & Numa, S. (1989) *Nature (London)* **340**, 230-233.
5. Mori, Y., Friedrich, T., Kim, M.-S., Mikami, A., Nakai, J., Ruth, P., Bosse, E., Hofmann, F., Flockerzi, V., Furuichi, T., Mikoshiba, K., Imoto, K., Tanabe, T. & Numa, S. (1991) *Nature (London)* **350**, 398-402.
6. Starr, T. V. B., Prystay, W. & Snutch, T. P. (1991) *Proc. Natl. Acad. Sci. USA* **88**, 5621-5625.
7. Williams, M. E., Feldman, D. H., McCue, A. F., Brenner, R., Velicelcebi, G., Ellis, S. B. & Harpold, M. M. (1992) *Neuron* **8**, 71-84.
8. Hui, A., Ellinor, P. T., Krizanova, O., Wang, J.-J., Diebold, R. J. & Schwartz, A. (1991) *Neuron* **7**, 35-44.
9. Dubel, S. J., Starr, T. V. P., Hell, J., Ahljanian, M. K., Enyeart, J. J., Catterall, W. A. & Snutch, T. P. (1992) *Proc. Natl. Acad. Sci. USA* **89**, 5058-5062.
10. Williams, M. E., Brust, P. F., Feldman, D. H., Patthi, S., Simerson, S., Maroufi, A., McCue, A. F., Velicelcebi, G. & Ellis, S. B. (1992) *Science* **257**, 389-395.
11. Snutch, T. P., Leonard, J. P., Gilbert, M. M., Lester, H. A. & Davidson, N. (1990) *Proc. Natl. Acad. Sci. USA* **87**, 3391-3395.
12. Perez-Reyes, E., Wei, X., Castellano, A. & Birnbaumer, L. (1990) *J. Biol. Chem.* **265**, 20430-20436.
13. Grabner, M., Friedrich, K., Knaus, H.-G., Striessnig, J., Scheffauer, F., Staudinger, R., Koch, W. J., Schwartz, A. & Glossmann, H. (1991) *Proc. Natl. Acad. Sci. USA* **88**, 727-731.
14. Koch, W. J., Ellinor, P. T. & Schwartz, A. (1990) *J. Biol. Chem.* **265**, 17786-17791.
15. Biel, M., Ruth, P., Bosse, E., Hullin, R., Stuhmer, W., Flockerzi, V. & Hofmann, F. (1990) *FEBS Lett.* **269**, 409-412.
16. Ahmad, S. N. & Miljanich, G. (1988) *Brain Res.* **453**, 247-256.
17. Sambrook, J., Fritsch, E. F. & Maniatis, T. (1989) *Molecular Cloning: A Laboratory Manual* (Cold Spring Harbor Lab., Plainview, NY).
18. Sanger, F., Nicklen, F. & Coulson, A. R. (1977) *Proc. Natl. Acad. Sci. USA* **74**, 5463-5467.
19. Devereaux, J., Haerberli, P. & Smithies, O. (1984) *Nucleic Acids Res.* **12**, 387-395.
20. Bean, B. P. (1989) *Annu. Rev. Physiol.* **51**, 367-384.
21. Anwyl, R. (1991) *Brain Res. Rev.* **16**, 265-281.
22. Niidome, T., Kim, M.-S., Friedrich, T. & Mori, Y. (1992) *FEBS Lett.* **308**, 7-13.
23. Stuhmer, W., Conti, F., Suzuki, H., Wang, X., Noda, M., Yahagi, N., Kubo, H. & Numa, S. (1989) *Nature (London)* **339**, 597-603.
24. Vassilev, P., Scheuer, T. & Catterall, W. A. (1988) *Science* **241**, 1658-1661.
25. Horne, W. A., Hawrot, E. & Tsien, R. W. (1991) *J. Biol. Chem.* **266**, 13719-13725.
26. Bennett, M. K., Calakos, N. & Scheller, R. H. (1992) *Science* **257**, 255-259.
27. Strong, M., Chandy, K. G. & Gutman, G. A. (1993) *Mol. Biol. Evol.* **10**, 221-242.
28. Salkoff, L., Baker, K., Butler, A., Covarrubias, M., Pak, M. D. & Wei, A. (1992) *Trends Neurosci.* **15**, 161-166.
29. Edmonds, B., Klein, M., Dale, N. & Kandel, E. R. (1990) *Science* **250**, 1142-1147.
30. Pelzer, S., Barhanian, J., Pauron, D., Trautwein, W., Lazdunski, M. & Pelzer, D. (1989) *EMBO J.* **8**, 2365-2371.
31. Tanabe, T., Beam, K. G., Adams, B. A., Niidome, T. & Numa, S. (1990) *Nature (London)* **346**, 567-569.